KES Transactions on Sustainable Design and Manufacturing I
Sustainable Design and Manufacturing 2014 : pp.703-719 : Paper sdm14-095

Design for Reliability of Half-Bridge Module due to Design Consideration and Material Selection

J. Eckermann[1], S. Mehmood, H.M. Davies, N. P. Lavery, S.G.R. Brown, J. Sienz[2]
A. Jones, P. Sommerfeld[3]

[1] Corresponding author email: J.Eckermann@swansea.ac.uk
[2] Advanced Sustainable Manufacturing Technologies (ASTUTE), College of Engineering, Swansea University, Singleton Park, Swansea, SA2 8PP, United Kingdom
[3] Electronic Motion Systems UK Lt d, Heol-y-Ddraig, Penllergaer Business Park, Penllergaer, Swansea SA4 9HL United Kingdom

Abstract

This paper primarily investigated the effect of the different half-bridge module layouts for Hybrid electric vehicle (HEV/EV) on the reliability. Throughout the investigations, computational simulations were carried out on two different simplified half-bridge modules. The viscoplastic constitutive model Anand was employed in this case to calculate the plastic strain in the solder under thermal shock cycling loading. The scope of the research was broadened by selecting the various solder materials, which were subjected to power and thermal shock cycle loading. Hereby, the material data from SAC105, SAC205, SAC305, SAC405 and Sn36Pb2Ag were chosen and implemented in Ansys. To reduce the computational time, 2D models replaced the 3D models. Additionally, metallurgical investigations were carried out to highlight any additional effects, which influenced the joint reliability.

Introduction

Designing for reliability is one of the key factors to avoid the massive warranty cost and to obtain customer satisfaction at a high level. This fundamental concept is also valid for half- bridge module used for HEV/EV. A solder joint failure in a half-

[1] Corresponding author email: J.Eckermann@swansea.ac.uk
[2] Advanced Sustainable Manufacturing Technologies (ASTUTE), College of Engineering, Swansea University, Singleton Park, Swansea, SA2 8PP, United Kingdom
[3] Electronic Motion Systems UK Ltd, Heol-y-Ddraig, Penllergaer Business Park, Penllergaer, Swansea SA4 9HL United Kingdom

bridge module is a serious incident. The use of the ideal substrate materials will positively influence the degree of solder joint stress-strain development when temperature changes [1] [2]. Using a proper thermal management system, the half-bridge module is able to survive the harsh test and operation conditions. Especially, solder suffers extremely from the impact of heat fluctuation due to the mismatch of the coefficient of thermal expansion (CTE) of the connected materials. Solders are metal alloys, which are fusible under a certain temperature, and in general, they are mechanically soft. Their microstructures are often unstable at operating temperatures due to the recrystallization processes, which can start at low temperature [3]. Solder alloys are used to join two parts together and to provide an electrical interconnection between the two parts [4]. Thermal stresses occur due to differences in CTEs of the metal parts and the solders. The lifetime of the solders will be reduced due either creep or/and fatigue mechanisms which also cause additional stresses in the solder. Creep is defined as a flow of material. Cracks growths and propagates happen in the fatigue mechanisms due to repeating mechanical loading. In thermal loading, both creep and fatigue mechanisms are the driven factors in reducing the lifetime of solders. At higher temperature, creep dominates over fatigue.

Soldering and wire bonding are two of the joining technologies [5] used in the power modules industry. In the past, solder was made with lead because it was a relatively cheap material and it is well suited for the application purpose. On the other hand, it is a toxic chemical element causing damage in the ecosystem when lead inside from electronic products leaches into the soil of the landfill [6]. Lead is classified as a hazard material and therefore “Restriction of Hazardous Substances Directive” has banned lead from electrical and electronic components since 1st July 2006 [6]. Tin-silver and copper (SAC) solder alloys were developed to replace lead solder alloys. It has become one of the most used solder alloys in the electronic industry [7] [8]. At present, the creep behaviour and lifetime expectation of these lead free solders are still poorly understood under the influence of temperature fluctuations. Therefore, much effort is being expended in time-consuming experimental investigations as well as simulation activities [9] to obtain data on the creep behaviour and the lifetime expectation.

The most common solder –substrate intermetallic compound is tin-copper (Sn-Cu). The interfacial Cu-Sn intermetallic compound (IMC) forms and grows during soldering as well as during their use. Within a few seconds, the solder closest to the copper surface is supersaturated with copper. As a result, intermetallic crystals with the composition Cu_6Sn_5 are precipitated on the copper surface [10] [11]. The newly formed layer has an uneven thickness between 0.5 and 2 µm. Crystals with Cu_3Sn are also formed at the Cu_6Sn_5/Cu interface, which is difficult to detect because of their thin layer [12] [13] [14] [15]. The amount of crystals Cu_3Sn can increase to 30-50% of the intermetallic layer after aging solder at temperature above 100◦C [16] [17] [18] [19]. A continuous layer of Cu_3Sn can be detected at a

thickness of 5-7 µm. Further studies about the effect of other elements on intermetallic layers are reported in [20] [21] [16] [22]. Intermetallic layer growths play a significant role in the solder joint reliability. Intermetallics are needed; however, it can lead to embrittled joints [23] and unsolderable components. Kirkendall void is a type of defects caused by impurities in the copper and it influences the reliability of the solder joints. Kirkendall void was not detected at high purity copper soldered with pure Sn or pure SnAgCu. However, it was observed at electrolytic and electroless deposited copper attached with Sn and SnAgCu solders [13].

A material subjected to a constant load or stress undergoes progressive plastic deformation over a period. This time dependent phenomenon is called creep. A classical creep curve is illustrated in Figure 1, which is divided into three regions, namely the primary creep, secondary creep and the tertiary creep. At the primary region, the initial high strain rate decelerates with increased time due to work hardening until it maintains almost constant. The secondary region begins where hardening and annealing is in balance. This region is well understood for many materials. In the tertiary creep region, the strain rate exponentially increases until the material will rupture [24].

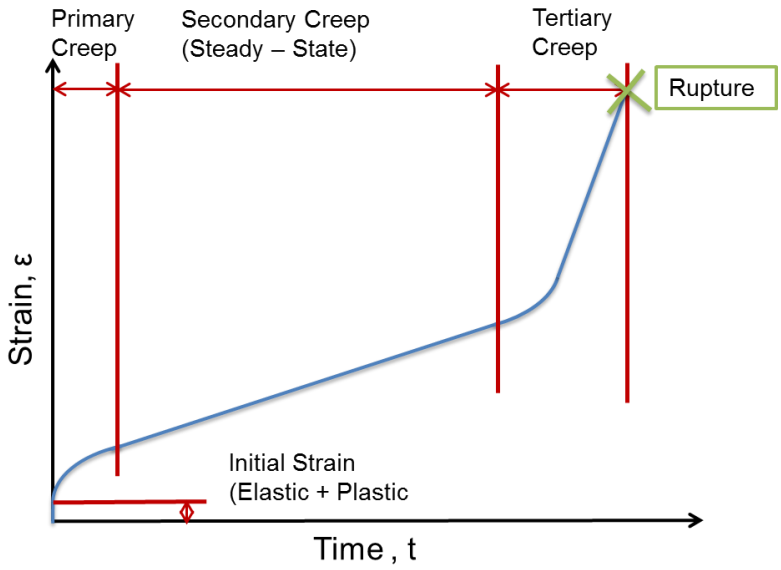

Figure 1: classical creep curve

Modelling methodology

Model designs

Modeling is an extremely useful tool in the early design stage. The advantages of modeling are the cost reduction in the product development and the reduction of project time as well as enhancement of engineering knowledge without experimental tests. The project aimed to obtain a better understanding of the effect of the design layout on product reliability. The emphasis was on simplifying the assembly model, which led to a model made of signal leads, power leads, solder and the electric board. 3D models were used to consider the cross-module bending moments. Two different layout versions A and B are illustrated in Figure 1. At Version A, one power lead is positioned between three signal leads on the left and three on the right in the back view. In the front view, there are two power signals at the left hand side and two signals leads on the right. In version B, there are seven signal leads in the back view and three power leads in the front view.

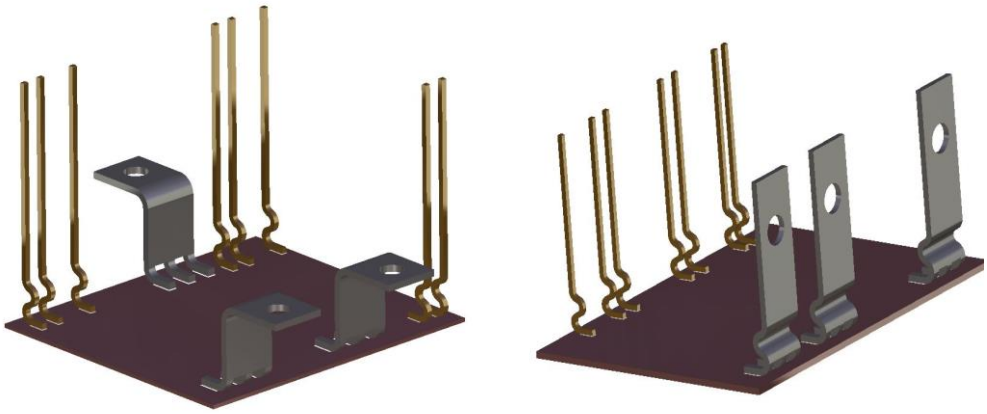

Figure 2: Simplified Designs for steering power module. Left: Version A and Right: Version B

A further simplification of modelling took place with the positive end effect of an additional reduction in computational time to make comparisons between various SAC and Lead – based solders. As illustrated in Figure 2, the simplified model consisted of only one signal lead, solder and copper board in a 2D model version and 3D model version.

Figure 3: 3D and 2 D models made of signal lead, solder and copper board

Anand is a viscoplastic constitutive model, which unified the plasticity and creep. This model is often chosen for characterising the thermal–mechanical behaviour of solders in electronic assemblies in FEA. Many previous simulations have been carried out with Anand constitutive model [4, 25]. It consists of a flow equation and three evolution equations. More details about the Anand constitutive model are explained in [9] [4].

Table 1: Anand parameters for various solders [12] [13]

Symbols	**Units**	**SAC105**	**SAC205**	**SAC305**	**SAC387**	**SAC405**	**Sn36Pb2Ag**
S_0	MPa	2.348	6.6	2.15	3.299	1.3	12.41
Q/R	K^{-1}	8076	8500	9970	9883	9000	9400
A	S^{-1}	3.772	500	17.994	15.773	500	4000000
ξ		0.995	4.3	0.35	1.067	7.1	1.5
m		0.445	0.16	0.153	0.367	0.3	0.303
h_0	MPa	4507.5	6100	1525.98	1076.9	5900	1379
S^	MPa	3.583	28.7	2.536	3.151	39.4	13.79
n		0.012	0.04	0.028	0.035	0.03	0.07
a		2.167	1.3	1.69	1.683	1.1	1.3

ANSYS workbench 14.0 was the chosen finite element program for simulating the thermal – mechanical behaviour of various types of solders including hypoeutectic lead-free solders SAC105, SAC205, SAC305, SAC405 and lead solder Sn-36Pb-2Ag. Temperature loadings “thermal power cycles (80 to 150 ^{o}C)” and “thermal shock cycles (-40 to 125 ^{o}C)” were employed to generate the thermal

stress in solder. The temperature profile for thermal power cycles (80 to 150 ^{o}C) followed a typical zigzag profile (as illustrated in Figure 3 on the left side) whose first ramp up rate of 700 C/s heats up the assembly from 80 °C to 150°C within 0.1s followed by a second cooling rate of 7 °C/s for 10s. For the thermal shock profile (shown in Figure 3 on the right side), the ramp rates for heating and cooling the assembly between the temperature extremes of -40°C and 125°C takes 15s. The dwell time for both extremes is 30 min.

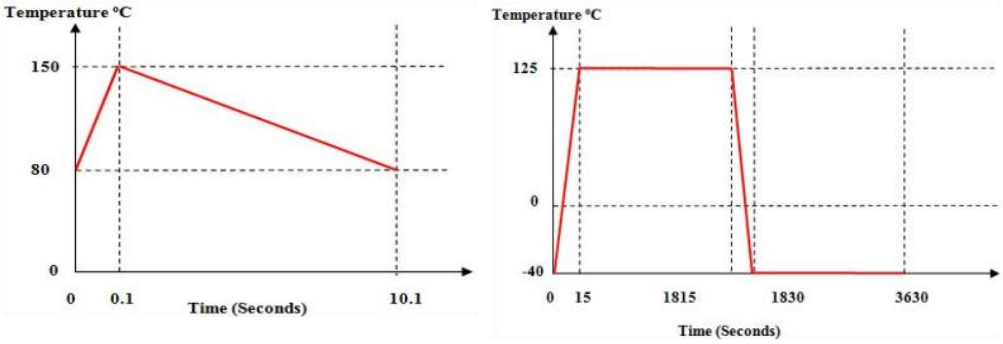

Figure 4: Power Cycle (80 to 150 ^{o}C) on the left and Thermal Shock Cycle (-40 to 125 ^{o}C) on the right

The type of mesh and the number of elements determine the degree of accuracy, the success of convergence and the duration of the simulation [26]. The 3D models were meshed structurally using a solid186 element. This higher order 3D element is defined by 20 nodes and allows to exhibit quadratic displacement behaviour [27].

The minimum number of sub steps was set at 5 and the maximum number was 20 for all load steps achievable by using the multistep function available in workbench 14.0. For the 2D model simulation, the higher order plane183 was selected with six notes element. The contact regions for all parts were set to be bonded. The bottom of the copper board has zero degree of freedom.

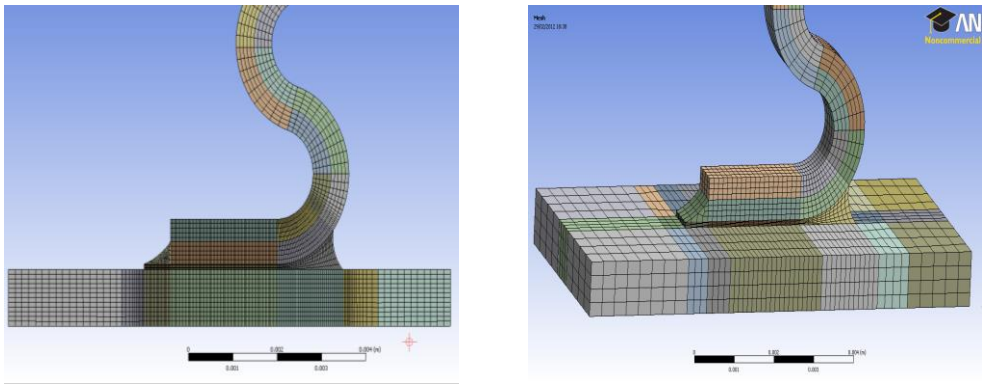

2D Model 3D Model

Figure 5: 2D and 3D models of Copper-Solder-Copper assembly

Experimental and Metallography

In this study, several lead signal – solder– board assemblies were fabricated and underwent thermal shock cycles. The thicknesses of the samples were similar to the industrial settings. Signal Lead and board was made of copper with 99.9% purity. SAC 305 made of 96.5% tin, 3% silver and 0.5% copper was used as a solder whose melting point is 217^{o} C [28]. The surfaces of the metallographic specimens were prepared by polishing before optical microscopy on Reichert MeF3 was carried out. Nikon camera DS-Fi1 with support of Nikon Elements D software captured the images.

Results

The simplified half-bridge modules Version A and Version B underwent five thermal shock cycles whose computational outcomes are illustrated in Figure 6. The picture on left illustrated the contour plot of plastic strain for Version A. The contour plot of the plastic strain for Version B can be seen on the left.

Figure 7 compared the version A to version B in terms of the maximum plastic strain in the signal lead and power lead. It was noticeable that the solder used for bonding the signal leads to the copper board performed around 20% higher plastic strain at version B. This would have significant impact to the lifetime of the solder. A numerical artifact can be seen at the first thermal shock cycle since the plastic strains for both signal leads are higher than the following ones which is practically

not possible. The reason is that plastic deformation is not able to recover after removing the loading.

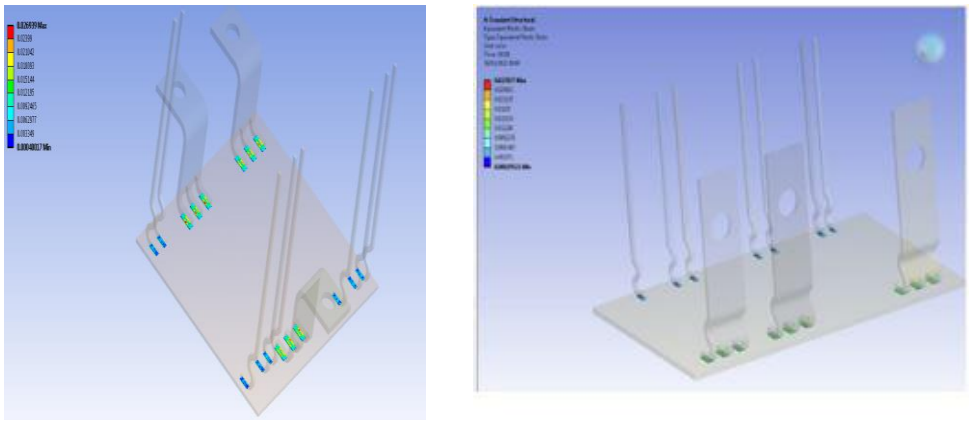

Figure 6: Plastic strain distributions in the solders in Version A (left) and Version B (right)

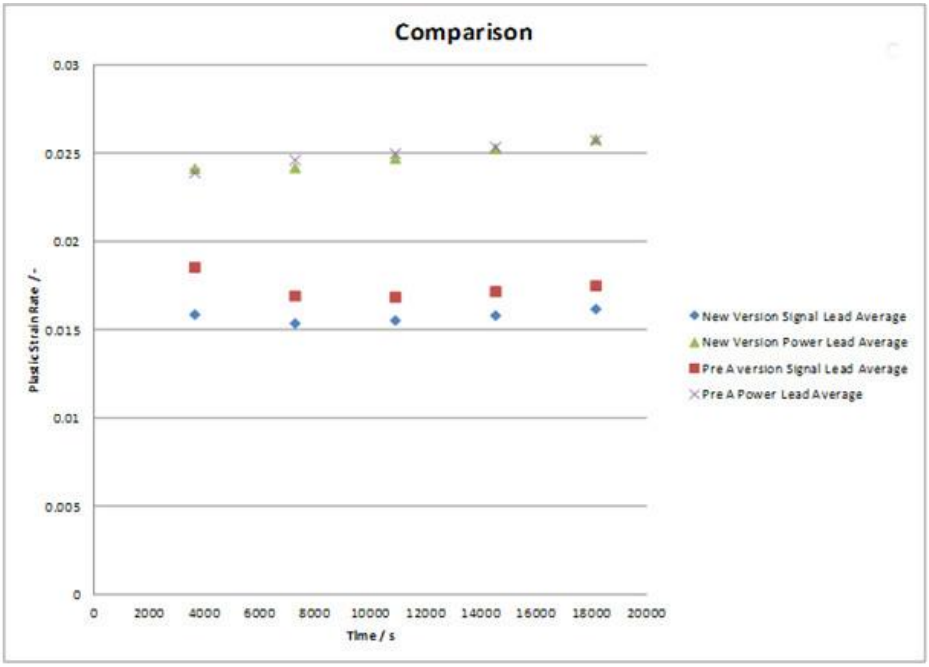

Figure 7: Comparison of the average plastic strain occurred in signal and power lead at version A and version B under thermal shock loading

To extend the knowledge about the impact of thermal shock cycle on the solder, further computational simulations were carried out with higher numbers of cycles on various type solders with 3D model and 2D model.

In Figure 8, the maximum plastic strain was plotted over number of thermal shocks. The plastic strain curves for SAC305 and Sn-36Pb-2Ag obtained with 3D model and 2D model are shown in this graph. The simulation for SAC 305 (2D) overestimated the plastic strain in compare to the 3D model, whereas, for Sn-36Pb-2Ag, the 3D model has a lower plastic strain value in compare to the 2D model. At 100 cycles, the maximum plastic strain of 1.86 occurred at SAC 305 (2D) is almost three times higher than the 3D Version (0.607). In the case of Sn-36Pb-2Ag, the 2D model shows almost 20% higher maximum strain rate in compare to the 3D model at the final cycle. This finding concludes that the 2D model has the tendency to calculate a higher strain rate as the 3D model, which needs to be considered for the lifetime calculations to avoid an underestimation.
At this stage, an explanation for this different result is not known and need further investigation.

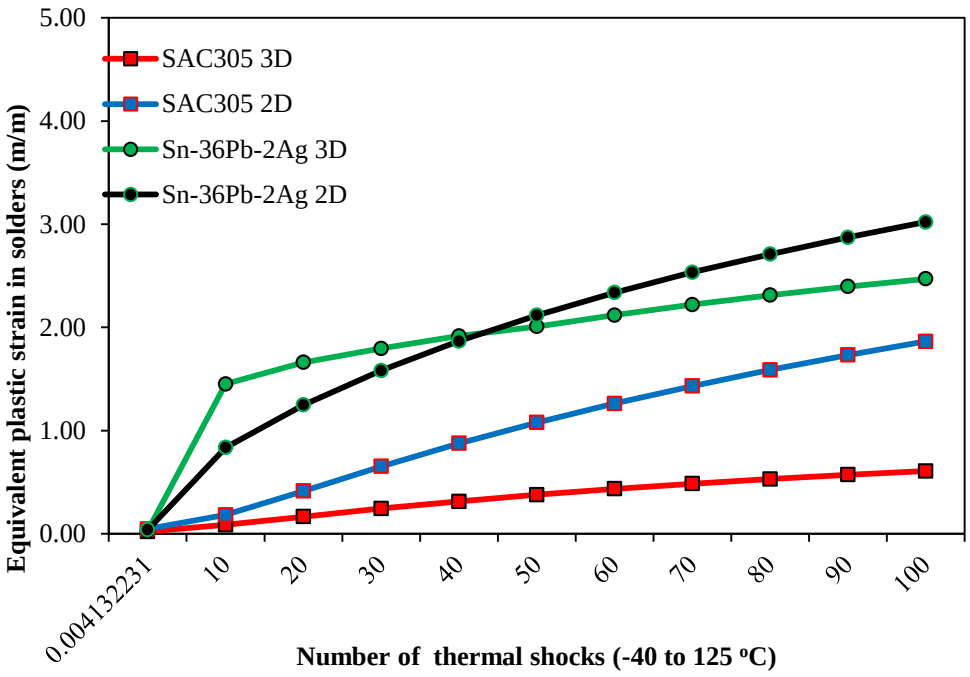

Figure 8: Comparison of maximum equivalent plastic strain between SAC305 and Sn-36Pb-2Ag over 100 thermal shocks cycles: (●) Sn-36Pb-2Ag (3D), (●) Sn-36Pb-2Ag (2D), (■) SAC305 (3D) and (■) SAC305 (2D))

With the consideration of the 2D overestimation, further simulations were carried out based on the 2D model principle to identify which type of solder exhibited the highest plastic strain resistance under the thermal shock conditions.

Figure 9 illustrated several plastic strain curves from SAC105, SAC205, SAC305, SAC405 and, Sn-36Pb-2Ag. The highest creep resistance can be found at SAC405 in contrast to Sn-36Pb-2Ag. The plastic strains of the solder alloys SAC105, SAC305, SAC387 and SAC405 are almost similar until around 400000 s where the plastic strain rate started to different for each solder. A well-deformed primary stage exits at all solders. The secondary stage is well defined at almost all solders except SAC305.

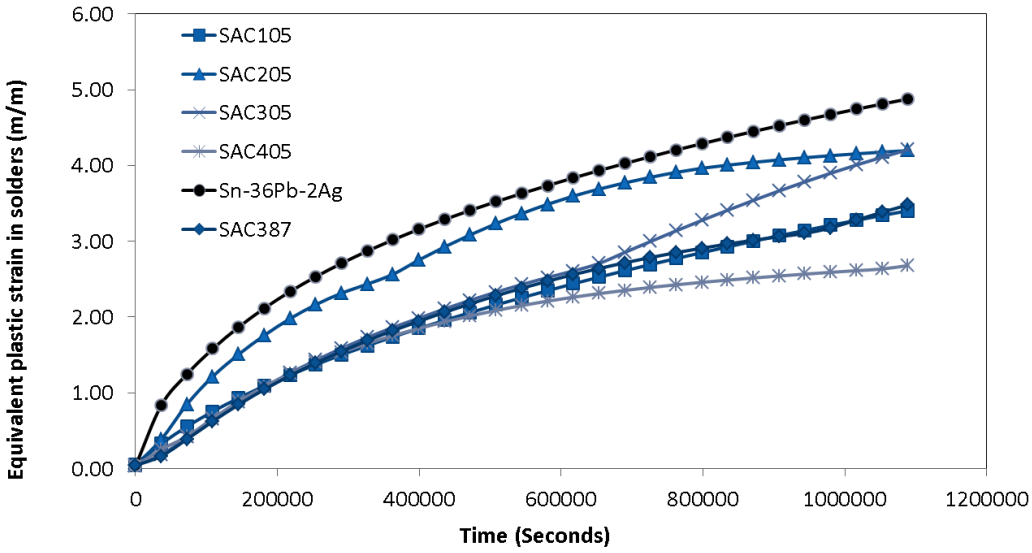

Figure 9: 2D Comparison of maximum equivalent plastic strain for various solders over time (300 cycles): Sn-36Pb-2Ag (●), SAC105 (■), SAC205 (▲), SAC305 (x), SAC387 (♦), SAC405 (*).

Additionally, a set of simulations was undertaken using power shock loading. In Figure 10, the outcomes of the simulations using Power cycles can be seen for various solders. As expected, the SN-36Pb-2Ag possessed the lowest plastic strain resistance. Surprisingly, SAC305 responded very well followed by SAC387 in terms of plastic strain resistance. The plastic strain of Sn-36Pb-2Ag at 300 cycles was around 4.5 times higher than the SAC305.

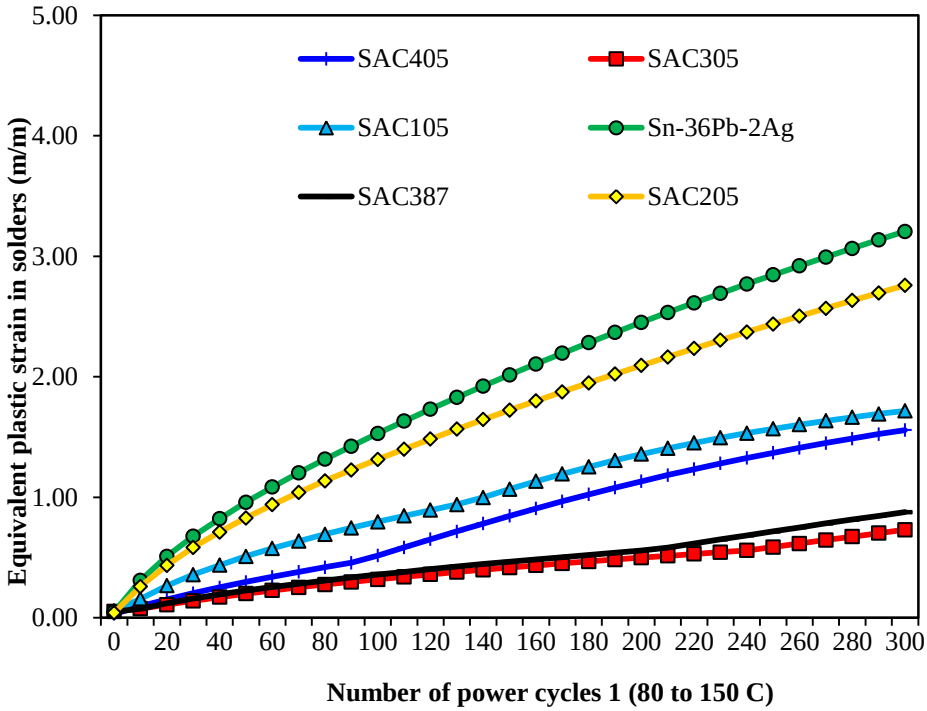

Figure 10: Equivalent plastic strain for various solders versus number of power cycle 1 (300 cycles). Data points are equivalent plastic strains obtained from Anand modeling for solders: Sn-36Pb-2Ag (●), SAC105 (▲), SAC205 (♦), SAC305 (■), SAC387 (-), SAC405 (+).

By analysing the evolution of plastic strain in the solder, it was noticed that the highest equivalent plastic strain always starts at the corner of the solder join and then the string vertically propagated.

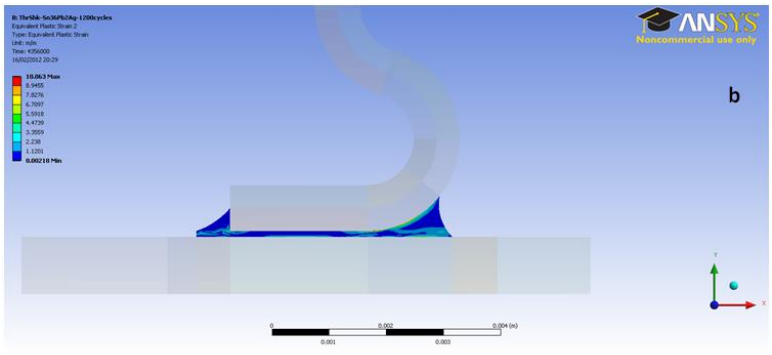

Figure 11- Contour plots after 1200 thermal shocks

Finally, the focus was to predict the optimal thickness of the solder. This result was shown in Figure 12 where the plastic strain is plotted over solder thickness. SAC305 was selected to calculate the ideal thickness at 10 cycles under thermal shock condition. A comparison between the 2D model and 3D model was also undertaken.

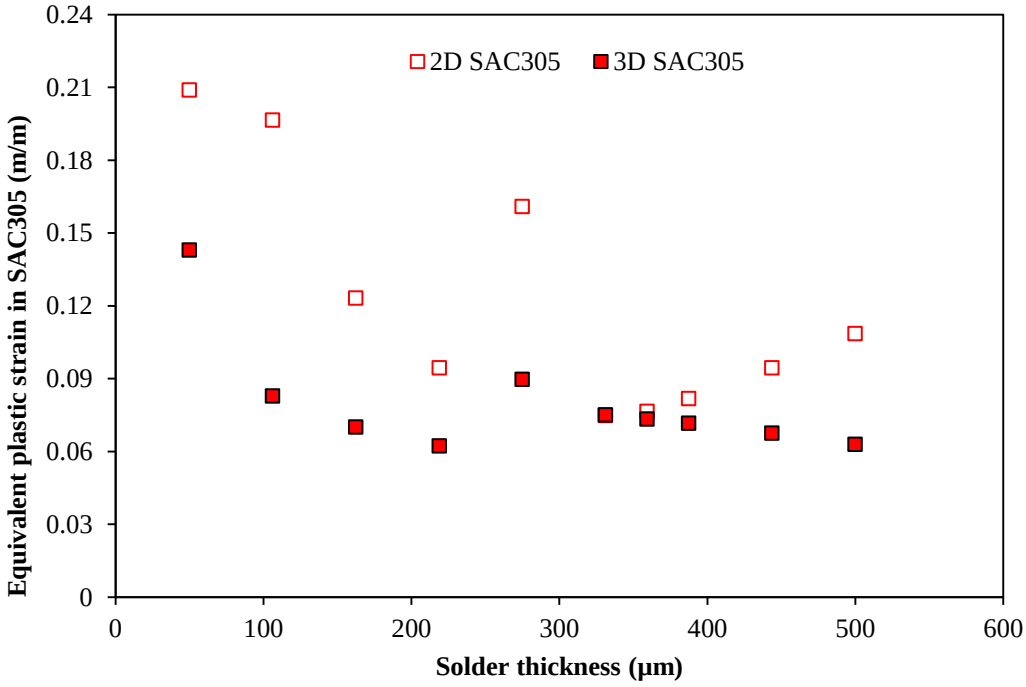

Figure 12: Optimization of solder thickness using 2D And 3D models

According to Figure 12, the ideal thickness seemed to be in the range 200-400 µm for 2D and 3D. Any dependencies of geometry and thermal condition on the ideal solder thickness are not known.

Metallurgy investigations were carried out to highlight any other effects, which would lead to a reduction of lifetime [29] [30]. The samples underwent thermal loading (thermal shock). Illustrated in
Figure 13, several materials related phenomenon occurred which will have a huge impact on the joint reliability. One of them was the formation of groove occurred at 100 cycles. Another one was Kirkendall voids formed after 300 cycles due to faster diffusion of Cu than Sn, which results in a formation of porous Cu/Cu_3Sn interface and Cu_3Sn layer.

At 450 cycles, Cu_3Sn IMC layers were visible behind Cu_6Sn_5 IMC layer. A degradation of IMC layer was detected at 600 cycles.

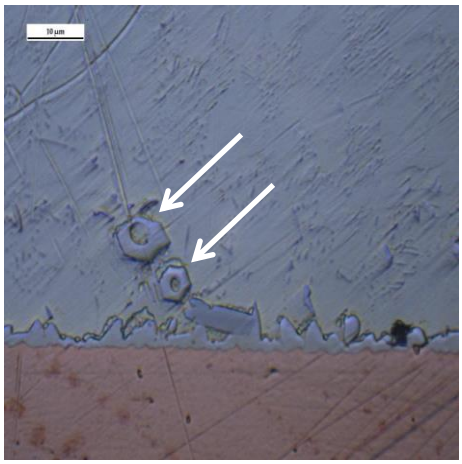

Formation of Kirkendall voids

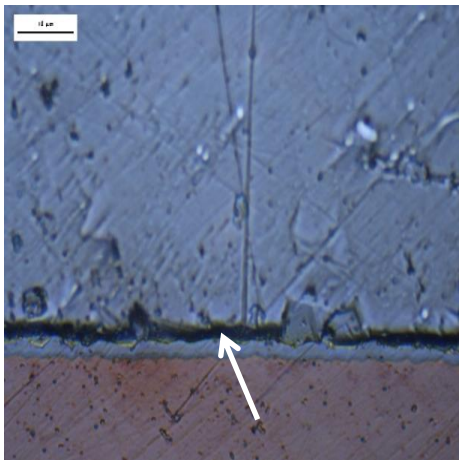

Occurrence of Groove

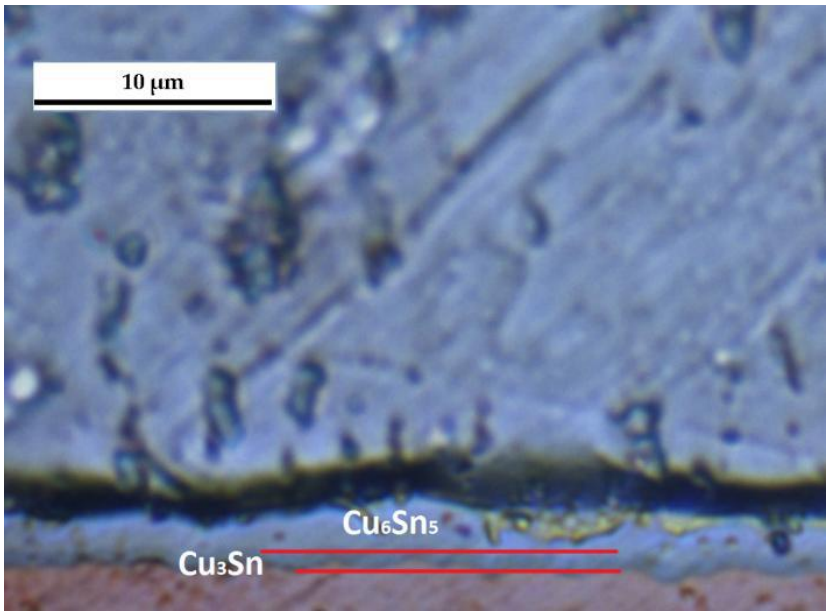

Formation of intermetallic Layers

Figure 13: Side view SEM images showing Kirkendall voids, Groove and intermetallic layers Cu_3Sn and Cu_6Sn_5

Conclusions

- The layout of signal lead and power lead significant affect the product reliability and therefore needs to be considered in the design phase.
- SAC405 has the highest creep resistance under thermal shock, whereas Sn-36Pb-2Ag performed the worst among the soldiers.
- In terms of the power cycle, SAC305 possesses the highest creep resistance, whereas SN-36Pb-2Ag shows the lowest creep resistance again.
- The ideal material would be SAC305 since the power cycles have a much higher impact on the joint reliability than thermal shock cycles [9].
- It is recommended that the solder thickness ranged between 200 µm and 400 µm.
- Degradation of ICM noticeable at 600 cycles
- Kirkendall voids reduced the joint reliability and is an indicator of the degree of impurity in the copper. To obtain a higher joint reliability, it is important to choose high quality of copper materials

Acknowledgments

The work described in this paper was carried out as part of the Advanced Sustainable Manufacturing Technologies (ASTUTE) project (ref. numb. 80380) in collaboration with Electronic Motion Systems, whom the authors would like to thank for their inputs. ASTUTE has been part-funded by the European Regional Development Fund through the Welsh Government, and the authors would like to acknowledge this funding.

BIBLIOGRAPHY

[1] A. De Angelis, "Companies and Markets," 21 April 2013. [Online]. Available: http://www.companiesandmarkets.com/News/Automotive-and-Parts/Electric-power-steering-industry-driven-by-the-increasing-demand-for-fuel-efficiency/NI7028. [Accessed 11 November 2013].

[2] W. J. Tomlinson and I. Collier, "The mechanical properties and microstructures of copper and brass joints soldered with eutectic tin-bismuth solder," Journal of Materials Science, vol. 22, pp. 1835-1839, 1987.

[3] Z. Mei and J. W. Morris, "Characterization of Eutectic Sn-Bi Solder Joints," Journal of Electronic Materials, vol. 21, pp. 599-600, 1992.

[4] D. L. McDowell, M. P. Miller and D. C. Brooks, "A Unified Creep-Plasticity Theory for Solder Alloys," ASTM International, 1994.

[5] G. Z. Wang, Z. N. Cheng, K. Becker and J. Wilde, "Applying Anand Model to Represent the Viscoplastic Deformation Behavior of Solder Alloys," Journal of Electronic Packaging, vol. 123, no. 3, pp. 247-253.

[6] M. Knoerr and A. Schletz, "Power Semiconductor Joining through Sintering of Silver Nanoparticles: Evaluation of Influence of Parameters Time, Temperature and Pressure on Density, Strength and Reliabiliy," in 6th International Conference on Integerated Power Electronic Systems, Nuernberg, 2010.

[7] M. Hangtao and J. Suhling, "A review of mechanical properties of lead-free solders for electronic packaging," Journal of material science, pp. 1141-1158, 2009.

[8] M. Abtew and G. Selvaduray, "Lead-free solders in microelectronics," Materials Science and Engineering, vol. 27, pp. 95-141, 2000.

[9] K. Zeng and K. N. Tu, "SNPb solder reactionin flip technolgoy," Materials Science and Engineering, pp. 55-111, 2002.

[10] J. Eckermann, S. Mehmood, N. P. Davies, N. P. Lavery, S. G. Brown, J. Sienz, A. Jones and P. Sommerfeld, "Computational modelling of creep-based fatigues as a means of selecting lead-free solder alloys," in EuroSime 2013 14th IEEE International Conference on Thermal, Mechanical and Multi-Physics Simulation and Experiments in Microelectronics and Microsystems, Wroclaw, 2013.

[11] V. Laurila, F. M. Vuorinen and J. K. Kivilahti, "Interfacial Reactions between Lead-free Solders and Common Base Materials," Materials Science and Engineering, vol. 49, no. 1-2, pp. 1-60, 2005.

[12] E. J. Cotts, R. Kinyanjui, R. Chromik, A. Zribi and P. Borgesen, "Formation of Intermetallic Compounds at Pb-Sn/Metal and Lead-Free/Metal Interfaces in Solder Joints," in Handbook of Lead-Free Solder Technology for Microelectronic Assemblies, New York, Marcel Dekker, 2004, p. Chapter 13.

[13] S. e. a. Terashima, "Effect of Silver Content on Thermal Fatigue Life of Sn - x Ag - 0.5Cu Flip - Chip Interconnects," Journal of ELECTRONIC MATERIALS, vol. 32, no. 12, pp. 1527-33, 2003.

[14] G. e. a. Henshall, "Comparison of Thermal Fatigue Performance of SAC105, Sn - 3.5Ag, and SAC305 BGA Components with SAC305 Solder Paste," in in Proc APEX, 2009.

[15] H. S. e. a. Ng, "Absolute and relative fatigue life prediction methodology for virtual qualification and design enhancement of lead free BGA," in Electronic Components and Technology Conference, 2005.

[16] K. e. a. Becker, "Applying anand model to represent the viscoplastic deformation behavior of solder alloys Journal of Electronic Packaging," Journal of Electronic Packaging, p. 123, 2001.

[17] R. E. Pratt, E. I. Stromsworld and D. J. Quesnel, "Effect of solid-state intermetallic growth on the fracture toughness of Cu/63Sn-37Pb solder joints," IEEE Transactions on Components, Packaging, and Technology, vol. 19, no. 1, pp. 134-141, 1996.

[18] P. G. Harris and K. S. Chaggar, "The Role of Intermetallic Compounds in Lead-free Soldering," Soldering and Surface Mount Technology, vol. 10, no. 3, pp. 38-52, 1998.

[19] P. T. Oberndorff, M. Dittes and L. Petit, "Intermetallic Formation in Relation to Tin Whiskers," in Proceedings of the IPC/Soldertec Global 1st International Conference on Lead Free Electronics, 2003.

[20] G. Xiao, P. Chan, C. Jian, A. Teng and M. Yuen, "The Effect of Cu Stud Structure and Eutectic Solder Electroplating on Intermetallic Growth and Reliability of Flip-Chip Solder Bump," in Proceedings of the 50th Electronic Components and Technology Conference, 2000.

[21] C. H. Toh, L. Hao , C. T. Tu and T. D. Chen, "Interfacial reactions in Ni-doped SAC105 and SAC405 Solders on Ni-Au Finish during Multiple Reflows," in 8th International Conference Electronic Packaging Technology, Shanghai, 2007.

[22] D. C. Lin, R. Kovacevic, T. S. Srivatsan and G. X. Wang, "A study aimed at characterizing the interfacial structure in a tin-silver solder on nicke-coated copper plate during aging," Sadhana, vol. 33, pp. 251-259, 2008.

[23] D. R. Frear, W. B. Jones and R. Kinsman, "Solder mechanics-a state of the art assessment," 1991.

[24] E. Tegehall, "Review of the impact of intermetallic layers on teh brittleness of tin-lead and lead-free solder joints," IVF, Moelndal, 2006.

[25] "Products-Sterring Power Module," Electronic Motion Systems, [Online]. Available: http://www.electronicmotionsystems.co.uk/products_4.htm. [Accessed 20 October 2013].

[26] Q. Wang, Y. Zhang, L. Liang, Y. Liu and S. Irving, "Anand Parameter Test for Pb-Free Material SnAgCu and Life Prediction for a CSP," Electronic Packaging Technology, pp. 1-9, 2007.

[27] S. Ridout and C. Bailey, "Review of Methods to Predict Solder Joint Reliability Under Thermo-mechanical Cycling," Fatigue and Fracture of Engineering Materials and Structures, vol. 30, no. 5, pp. 400-412, 2007.

[28] A. Syed, "Updated Life Prediction Models For Solder Joints With Removal of Modelling Assumptions and Effects of Constitutive Equations," in 7th International Conference on Thermal, Mechanical and Multiphysics Simulation and Experiments in Micro-Electronics and Micro-Systems, EuroSime 2006, 2006.

[29] I. E. Anderson, "Development of Sn-Ag-Cu and Sn-Ag-Cu-X alloys for Pb-free electronci solder applications," Journal of Material Science-Materials in Engineering, vol. 18, pp. 55-76, 2007.

[30] I. Siti Rabiatull Aisha, A. Ourdjini, A. Astuty and O. Saliza Azlina, "Effect of silver content on intermetallics formation on copper and immersion silver surface finishes," in 2nd International Conference on Green Technology and

Engineering , Malahayati, 2009.

[31] X. P. Li, J. M. Xia, M. B. Zhou, X. Ma and X. P. Zhang, "Solder volume effects on the microstructure evolution and shear fracture behaviour of ball grid array structure Sn-3.0Ag-0.5Cu solder interconnects," Journal of Electronic Materials, vol. 40, no. 12, pp. 2425-2435, 2011.

[32] C. Lea, A scientific guide to surface mount technology, Electrochemical Publications Ltd., 1988.

[33] P. Roubaud, G. Ng, G. Henshall, R. Bulwith, R. Herbet, S. Prasad, F. Carson, S. Kamath and A. Garcia, "Impact of Intermetallic Growth on teh Mechanical Strength of Pb-Free BGA Assemblies," in Proeedings of the APEC Conference , 2001.